HHS Public Access

Author manuscript

Cell Microbiol. Author manuscript; available in PMC 2019 June 01.

Published in final edited form as:

Cell Microbiol. 2018 June ; 20(6): e12828. doi:10.1111/cmi.12828.

Association of *Vibrio cholerae* 569B outer membrane vesicles with host cells occurs in a GM1-independent manner

Elnaz S. Rasti[1], **Megan L. Schappert**[1], and **Angela C. Brown**[1,*]

[1]Department of Chemical and Biomolecular Engineering, Lehigh University, Bethlehem, PA, USA

Summary

The primary virulence factor of *Vibrio cholerae*, cholera toxin (CT), initiates a pathway in epithelial cells that leads to the severe diarrhea characteristic of cholera. Secreted CT binds to GM1 on the surface of host cells to facilitate internalization. Many bacterial toxins, including CT, have been shown to be additionally delivered via outer membrane vesicles (OMVs). A fraction of the closely related heat labile toxin (LT) produced by enterotoxigenic *Escherichia coli* (ETEC) has been demonstrated to reside on the surface of OMVs, where it binds GM1 to facilitate OMV internalization by host cells. In this work, we investigated whether OMV-associated CT is likewise trafficked to host cells in a GM1-dependent mechanism. We demonstrated that a majority of CT is secreted in its OMV-associated form, and is located exclusively inside the vesicle. Therefore, the toxin is unable to bind GM1 on the host cell surface, and the OMVs are trafficked to host cells in a GM1-independent mechanism. These findings point to a secondary, noncompeting mechanism for secretion and delivery of CT, beyond its well-studied secretion via a type II secretion system and underscores the importance of focusing future studies on understanding this GM1-independent delivery mechanism to fully understand *V. cholerae* pathogenesis.

1 Introduction

The Gram-negative bacterium, *Vibrio cholerae*, is the causative agent of cholera, a severe diarrheal infection transmitted through the ingestion of contaminated food or water (Reidl & Klose, 2002). Because of the organism's highly virulent nature, severe outbreaks are common. Most recently, an ongoing outbreak in Yemen has affected at least 300,000 people, with an increasing death toll of around 1,700 patients (Balakrishnan, 2017), and the more than seven-year long outbreak in Haiti has killed over 10,000 people (Ivers, 2017).

Along with toxin-coregulated pilus (TCP), CT is one of the primary virulence factors produced by pathogenic strains of *V. cholerae* (Faruque, Albert, & Mekalanos, 1998; Matson, Withey, & DiRita, 2007). CT is a member of the AB class of bacterial toxins with a heterodimeric A subunit (CTA1/CTA2) and a homo-pentameric B subunit (CTB5) (Beddoe, Paton, Le Nours, Rossjohn, & Paton, 2010; Sanchez & Holmgren, 2011). CT is secreted through a two-step, type II secretion (T2S) system (Sandkvist, 2001a, 2001b; Sandkvist et al., 1997; Sikora, 2013). In the first step, the A and B subunits are translocated across the inner (cytoplasmic) membrane, in a Sec-dependent process. Once in the periplasmic space,

*Corresponding author: acb313@lehigh.edu, Tel. (+610) 758-4042, Fax. (+610) 758-5057.

the subunits are assembled into the holotoxin through the formation of disulfide bonds, catalyzed by the TcpG disulfide oxidoreductase. Finally, the extracellular protein secretion (Eps) apparatus recognizes the B5 pentamer of the assembled holotoxin to facilitate secretion across the outer membrane (OM) (Peek & Taylor, 1992; Sikora, 2013; Yu, Webb, & Hirst, 1992). After secretion, the B5 subunit of the CT holotoxin recognizes and binds to the GM1 ganglioside receptor on the surface of small intestinal epithelial cells, triggering endocytosis of the GM1-CT complex. The toxin is then transported to the endoplasmic reticulum (ER), where the enzymatic fragment of the CTA subunit dissociates from the holotoxin and unfolds (Taylor, Banerjee, Ray, Tatulian, & Teter, 2011) before retro-translocating to the cytosol where it activates adenylate cyclase (AC). This activation results in an increase in cytosolic cAMP, which in turn leads to diarrhea by means of an excessive release of water and chloride into the intestinal lumen (Chinnapen, Chinnapen, Saslowsky, & Lencer, 2007; Lencer, Delp, Neutra, & Madara, 1992; Lencer, Hirst, & Holmes, 1999; Spangler, 1992; Wernick, Chinnapen, Cho, & Lencer, 2010).

Like other Gram-negative bacteria, *V. cholerae* produces OMVs (Elluri et al., 2014; Mondal et al., 2016), and a recent study has demonstrated that physiologically active CT is found in association with these vesicles (Chatterjee & Chaudhuri, 2011). OMVs are naturally released spherical buds of the OM with an enveloped periplasmic content. These vesicles carry selective cargo, either associated with their membrane bilayer or encapsulated within their lumen, including DNA, RNA, proteins, lipids, and lipopolysaccharide (LPS). OMVs secreted from Gram-negative pathogens have been proposed to act as vehicles for delivering active toxins and other virulence factors to distant host cells (Bonnington & Kuehn, 2014; Kulp & Kuehn, 2010; Schwechheimer & Kuehn, 2015).

OMVs use a variety of mechanisms to enter host cells and deliver their cargo (Kaparakis-Liaskos & Ferrero, 2015; O'Donoghue & Krachler, 2016). Cholesterol-rich lipid rafts have been commonly reported to be involved in the uptake of OMVs produced by a number of species, including enterotoxigenic *Escherichia coli* (ETEC), *Haemophilus influenzae*, *Campylobacter jejuni*, and *Pseudomonas aeruginosa*, among others (Bomberger et al., 2009; Elmi et al., 2012; Kaparakis et al., 2010; Kesty, Mason, Reedy, Miller, & Kuehn, 2004; Mondal et al., 2016; Sharpe, Kuehn, & Mason, 2011), while OMVs produced by other organisms, including *Helicobacter pylori* and enterohemorrhagic *E. coli* (EHEC), have been reported to enter cells in cholesterol-independent endocytic processes (Bielaszewska et al., 2017; Bielaszewska et al., 2013; Canas et al., 2016; Kunsmann et al., 2015; Parker, Chitcholtan, Hampton, & Keenan, 2010).

The role of OMV-associated toxins in the trafficking and internalization of OMVs likewise seems to vary by organism. Delivery of some OMVs occurs through a toxin-receptor-independent mechanism (Bielaszewska et al., 2013; Elluri et al., 2014; Kunsmann et al., 2015); however, the uptake of ETEC OMVs has been reported to be facilitated by the interaction of vesicle-associated heat-labile enterotoxin (LT) with its GM1 ganglioside receptor (Kesty et al., 2004). LT is closely related to CT in both structure and biological activity, including its secretion through a T2S pathway and recognition of GM1 on the host cell (Tauschek, Gorrell, Strugnell, & Robins-Browne, 2002). We hypothesized that due to the similarity between LT and CT, vesicle-associated CT might also act as a targeting moiety

for OMVs, triggering host cell entry of the OMVs through binding to the toxin's cellular receptor, GM1. It has been proposed that the affinity of LT for LPS, found on the outer surface of the OMVs, regulates the cellular uptake of ETEC OMVs by allowing LT-receptor (GM1) binding (Horstman & Kuehn, 2002). Therefore, in the present work, we conducted a series of experiments to characterize the location of CT in *V. cholerae* 569B OMVs and to determine the role of GM1 in the interaction of the OMVs with host cells.

2 Results

2.1 Isolation and characterization of *V. cholerae* OMVs

We first investigated the secretion of OMVs by CT-expressing *V. cholerae* strain 569B. The culture was grown in nutrient broth until the late logarithmic phase to avoid contamination of the OMVs with lysed cell debris, and the OMVs were purified from the cell-free supernatants. Scanning electron microscopy (SEM) images of the OMVs exhibited spherical vesicles with diameters ranging from 60 to 250 nm (Fig. 1A). Dynamic light scattering (DLS) was used to determine that the average diameter of the 569B OMVs was 198.5 nm with a polydispersity of 0.292.

To determine whether CT is associated with 569B OMVs, Western blot analysis was performed using a polyclonal anti-CT antibody. Two strong antibody-reactive bands were found, with molecular weights of approximately 29 kDa and 18 kDa, confirming that the toxin is associated with the OMVs (Fig. 1B). We then used a dot blot analysis (Fig. S1) to determine what fraction of protein in the OMV is CT (mass CT/total protein mass). Purified 569B OMVs were spotted onto a nitrocellulose membrane along with a serial dilution of CT with known mass. The blot was then incubated with an anti-CT polyclonal antibody, and the intensity of the OMV dots was compared to the intensity of the CT dots to calculate the mass of CT in the OMVs. The total protein concentration of the OMVs was measured by collecting the absorbance at a wavelength of 280 nm (A280) on a Nanodrop™ spectrophotometer. This allowed us to calculate that CT comprised 0.5% of the total protein content of the vesicles.

To measure the fraction of secreted CT in the supernatant that is associated with OMVs, both isolated OMVs and the OMV-free supernatant were spotted on nitrocellulose along with purified CT in a serial dilution (Fig. 1C). We found that, by mass, 75% of the secreted CT is associated with vesicles, while only 25% of the secreted CT is in a free, soluble form.

2.2 OMVs induce morphological changes in host cells

To verify that the OMVs are biologically active, we tested 569B OMV-mediated cytotoxicity. A previous study has shown that CT treatment of FHs 74 intestinal epithelial cells induces a dose-dependent morphological change from an elongated (spindly) to a rounded form (Jin et al., 2013). We found that the 569B OMVs induced a similar effect on cells in a dose-dependent manner (Fig. 2A), demonstrating the biological activity of the OMVs. The cell morphology was scored on a scale of 1 (spindly) to 4 (round); quantification of the images in Fig. 2A is shown in Fig. 2B.

To compare the cytotoxicity of purified OMVs with the OMV-free supernatant, cells were treated with the same volume of OMVs and OMV-free supernatant, and the resulting cell rounding was quantified. As shown in Fig. 2C, the OMV fraction induced a greater cellular response than the supernatant. Representative images used for quantification in Fig 2.C are presented in Fig. S2.

2.3 CT does not have affinity for *V. cholerae* O1 LPS

The related toxin, LT, has been shown to reside partially on the surface of ETEC OMVs due to its affinity for LPS, which comprises the outer leaflet of the OMV (Horstman & Kuehn, 2002). We therefore sought to investigate the affinity of CT for the lipids comprising the OMV, using two lipid dot blot analyses. In the first blot, we investigated the affinity of CT for the OMV lipids, 1-palmitoyl-2-oleoyl-*sn*-glycero-3-phosphoethanolamine (POPE), 1-palmitoyl-2-oleoyl-*sn*-glycero-3-phospho-(1′-rac-glycerol) (POPG), tetraoleoyl cardiolipin (TOCL), and LPS, along with GM1. The affinity of CT for GM1 has previously been measured to be 4.6×10^{-12} by surface plasmon resonance (SPR) (Kuziemko, Stroh, & Stevens, 1996) and 5.2×10^{-8} by isothermal titration calorimetry (ITC) (Masserini, Freire, Palestini, Calappi, & Tettamanti, 1992). In our dot blot containing GM1 (Fig. 3A, i), we likewise observed a strong affinity of CT for GM1, and only a slight affinity for POPE and TOCL; no affinity for 569B LPS or POPG was detected. This result demonstrates that any affinity of CT for OMV lipids is significantly weaker than the toxin's affinity for GM1. In a second dot blot, we investigated the affinity of CT for only the OMV lipids, POPE, POPG, TOCL, and LPS; no GM1 was included in this blot so that we could compare the affinity of CT specifically for OMV lipids. In the absence of GM1, we observed some affinity of CT for POPE, very slight affinity for POPG and TOCL, and no affinity for 569B LPS (Fig. 3A). These results demonstrate that while CT has some affinity for the OMV lipid, POPE, this affinity is significantly weaker than the toxin's known strong affinity for GM1. Phosphatidylethanolamine (PE) lipids comprise a majority of the inner leaflet of the OM and likely that of the OMV as well, while LPS is located exclusively in the outer leaflet of the OM and OMV. Thus, this result suggests that, unlike LT, the association of CT with OMVs is not driven by an affinity for the outer surface of the vesicle. The LPS structure of the purified 569B LPS was verified by sodium dodecylsulfate polyacrylamide gel electrophoresis (SDS-PAGE) analysis (Fig. 3B).

2.4 CT is located within the lumen of OMVs

To determine the location of CT relative to the OMVs, a proteinase K susceptibility assay was carried out in the absence or presence of the membrane disrupting agent, SDS. As shown in Fig. 4A, vesicles that have not been treated with either proteinase K or SDS (lane 1) display a strong, antibody-reactive band along with two fainter bands. After proteinase K digestion (lane 2), the bands remain identical to those of the untreated OMVs. When the vesicles are first disrupted with SDS and then treated with proteinase K (lane 3), the faint bands disappear and the strong band is greatly diminished, indicating digestion of the CT. This result suggests that OMV-associated CT is inaccessible to proteinase K, thus likely within the vesicle lumen.

To further investigate the location of the toxin, we developed an indirect non-competitive ELISA in which a Nunc-Immuno plate was coated with a serial dilution of intact or EDTA-treated OMVs. Each well contained OMVs carrying 20 to 160 ng CT. In this assay, the anti-CT polyclonal antibody can only bind exposed CT molecules; thus, any intravesicular CT will not be detected. As shown in Fig. 4B, no antibody binding to intact vesicles was detected, indicating that CT is not present on the surface of the OMVs. However, a dose-dependent increase in antibody binding was observed for vesicles disrupted by EDTA, due to the release of CT packaged into the lumen of the vesicles. Together, these results indicate that OMV-associated CT is located entirely within the vesicles, rather than on the surface.

2.5 Association of OMVs with host cells is not GM1-dependent

The intravesicular location of CT suggests that the toxin would be unable to bind to its GM1 receptor on host cells. To determine if this so, a GM1 ELISA was performed using a serial dilution of CT as a standard. GM1 was coated on the plate, and either soluble CT or purified 569B OMVs were added in varying amounts. As expected, soluble CT bound strongly to coated GM1, and pre-incubation of the toxin with GM1 inhibited this binding (Fig. 5A). Surprisingly, neither untreated nor GM1-pretreated OMVs exhibited any binding to the GM1-coated wells (Fig. 5B), indicating that, unlike soluble CT, OMV-associated CT does not bind to GM1.

We next investigated whether pre-incubation of OMVs with GM1 would inhibit vesicle-mediated cytotoxicity. Both untreated and GM1-treated OMVs induced a similar morphological change in human FHs 74 Int cells (Fig. 5C, i and ii, respectively), resulting in similar cytotoxicity scores (Fig. 5D). This finding is consistent with the lack of GM1 binding by 569B OMVs.

To further analyze the role of GM1 in vesicle-host cell interaction, host cells were treated with FITC-OMVs or FITC-OMVs that were pre-incubated with GM1. As shown in Fig. 6, both untreated and GM1-treated OMVs were found to be associated with the host cells within two hours, demonstrating that OMV association to FHs74 Int cells occurs through a GM1-independent mechanism.

3 Discussion

CT, the primary virulence factor of *V. cholerae*, is secreted like its close relative, LT, through a two-step T2S process (Sandkvist, 2001a, 2001b; Sandkvist et al., 1997; Sikora, 2013; Tauschek et al., 2002) and is also associated with OMVs (Chatterjee & Chaudhuri, 2011). To date, a majority of studies about CT delivery to host cells have focused on the toxin's water-soluble form, in which it utilizes the GM1 receptor on the surface of the host cell to initiate endocytosis. In the present study, we demonstrated that most of the CT secreted by *V. cholerae* 569B is associated with OMVs and is physiologically active. We then investigated whether CT-containing OMVs are trafficked to host cells via the GM1 receptor in a similar manner as soluble CT.

We first investigated the localization of CT in the OMVs, hypothesizing that the toxin must be located on the surface of the OMVs to mediate OMV binding to GM1. However, unlike

LT, we found that CT has no affinity for LPS, which comprises the outer surface of the OMV, and is located entirely within the lumen of the vesicles. We then demonstrated that the host cell association of CT-containing 569B OMVs occurs through a mechanism that is independent of the GM1-CT interaction.

This finding is in contradiction with a previous report about OMVs produced by a different strain of *V. cholerae*, O395, (Chatterjee & Chaudhuri, 2011), in which they found that soluble GM1 inhibits OMV-mediated cAMP production and cytotoxicity, although they did not directly measure binding of the OMVs to GM1. This difference may be due to strain-to-strain variations in CT secretion, OMV production, and/or LPS structure. Although both strains belong to the O1 serogroup, O395 belongs to the Ogawa serotype (Shaw & Taylor, 1990), while 569B belongs to the Inaba serotype (Stroeher, Karageorgos, Morona, & Manning, 1992). These two serotypes are defined by variations in the structure of the O-antigen of LPS (Hisatsune, Kondo, Isshiki, Iguchi, & Haishima, 1993; Ito, Higuchi, Hirobe, Hiramatsu, & Yokota, 1994; Villeneuve, Boutonnier, Mulard, & Fournier, 1999). Thus, it is possible that although CT is present only in the lumen of 569B OMVs because it has no affinity for the LPS of this strain, CT may have an affinity for O395 LPS, allowing the toxin to reside on the surface of OMVs from the O395 strain, where it is able to bind GM1 on host cells.

The dispensability of toxins for cellular uptake of OMVs has been observed in other studies. EHEC hemolysin, *V. cholerae* cytolysin, and cytolethal distending toxin (CDT) expressed by *Aggregatibacter actinomycetemcomitans* and *Campylobacter jejuni* are a few examples of other OMV-associated virulence factors that are delivered to the host cell through a toxin-independent mechanism (Bielaszewska et al., 2013; Elluri et al., 2014; Elmi et al., 2012; Lindmark et al., 2009; Rompikuntal et al., 2012). Notably, Shiga toxin (Stx2a), the key virulence factor responsible for cytotoxicity of OMVs released from *E. coli* O104:H4, is another AB5 toxin, which, like CT, is located within the lumen of the OMV, thus protected from enzymatic degradation, and inaccessible to its globotriaosylceramide (Gb3) receptor (Kunsmann et al., 2015). On the other hand, as previously mentioned, LT, also an AB5 toxin, is found on the surface of ETEC OMVs and regulates OMV binding to the GM1 receptor (Horstman & Kuehn, 2002; Kesty et al., 2004). However, an extravesicular localization does not necessarily indicate that the toxin is involved in the cellular uptake of OMVs. For example, the leukotoxin (LtxA) produced by *Aggregatibacter actinomycetemcomitans,* although enriched in the outer surface of OMVs (Kato, Kowashi, & Demuth, 2002), is not required for vesicle delivery (Demuth, James, Kowashi, & Kato, 2003).

The lack of affinity of free CT for LPS and its absence on the outer surface of the OMVs suggests that CT secreted through the T2S system does not have any further interaction with OM of the bacteria or its secreted vesicles and will only bind to the GM1 receptor to be taken up by the host cell. Our results instead point to a mechanism in which, during the T2S process, instead of being transported from the periplasmic space across the OM of the bacteria, some CT becomes entrapped in the bacterial periplasm, allowing its incorporation in the lumen of the OMVs, thus offering an additional secretory pathway for CT (Fig. 7). Thus, we propose that *V. cholerae* 569B employs two different, non-competing mechanisms for the delivery of biologically active CT, one relying on GM1 for cellular uptake of free CT

and another in which OMV-associated CT is delivered via a GM1-independent mechanism. Our results demonstrate the need for studies detailing the mechanism of OMV-associated CT delivery to host cells to fully characterize delivery of this important virulence factor.

4 Experimental procedures

4.1 Chemicals

POPE, POPG, and TOCL were purchased from Avanti Polar Lipids (Alabaster, AL). Monosialoganglioside GM1 from bovine brain and CT were purchased from Sigma-Aldrich® (St. Louis, MO).

4.2 Strains and culturing conditions

The CT-expressing *V. cholerae* strain 569B (O1 biotype El Tor serotype Inaba, ATCC® 25870™) was used in this study. The culture was grown in nutrient broth at 37°C with aeration.

Human fetal small intestinal FHs 74 Int cells (ATCC® CCL241™) were cultured in Hybri-care medium (ATCC 46-X™), supplemented with 30 ng/mL epidermal growth factor (EGF, Sigma-Aldrich®) and 10% fetal bovine serum (Sigma-Aldrich®) at 37°C, with 5% CO_2. The medium was changed every two to three days.

4.3 Vesicle purification

OMVs were isolated from *V. cholerae* as described previously (Schild, Nelson, & Camilli, 2008), with some modifications. Briefly, after reaching the late logarithmic phase (OD_{600} of 1.0), the culture was centrifuged (10,000 × *g*, 10 min, 4°C), and the supernatants were filter-sterilized through a 0.45-um pore size filter. The supernatant was concentrated approximately 20-fold using an Amicon Ultra-15 centrifugal filter device with a 50 kDa molecular weight cut-off (Millipore). The final supernatant was subjected to ultracentrifugation (140,000 × *g*, 3 h, 4°C) using a Beckman SW 28 Ti rotor. The OMV pellet was washed with sterile phosphate-buffered saline (PBS), ultracentrifuged again, and resuspended in PBS. The sample was stored at 4°C and used within a week.

4.4 SEM

Purified OMVs were loaded on a plasma-cleaned glass coverslip (12 mm diam., Ted Pella) and dried overnight. After being fixed in Karnovsky's fixative for 2 hr, the samples were sequentially dehydrated with solutions of 35%, 70%, 85%, 95%, and 100% (v/v) ethanol in ddH_2O for 5 min each. The samples were further dehydrated with a 1:1 solution of ethanol: hexamethyldisilazane (HMDS) (2 × 15 min) followed by 100% HMDS (2 × 15 min), and then were allowed to air dry overnight. The dried samples were coated with iridium prior to imaging with a Hitachi 4300 SE/N at an accelerating voltage of 5 kV.

4.5 DLS

The size of the OMVs was measured by DLS using an ALV/CGS-3 goniometer system. A CONTIN analysis was used to determine the radius. The average diameter (z-average) and

size distribution (polydispersity index: PDI) of the OMVs were calculated by the cumulants method at 25°C with a laser at a wavelength of 632.8 nm under a scattering angle of 90°.

4.6 Western blot analysis

To characterize the presence of CT in the vesicles, 569B OMV proteins were separated by SDS-PAGE on an 8–16% mini-protean TGX precast protein gel (BioRad). Subsequently, the proteins were electrotransferred to a nitrocellulose membrane for 30 min at 30 V. The membrane was immersed in blocking buffer (5% non-fat dry milk in TBST), and then incubated with primary antibody (rabbit anti-CT: polyclonal, 1:5000, Abcam) followed by a secondary antibody (goat anti-rabbit immunoglobulin G conjugated to horseradish peroxidase (HRP), 1:5000, Southern Biotech). The CT bands were detected using SuperSignal™ enhanced chemiluminescent (ECL) substrate (Thermo Scientific™).

4.7 Calculation of CT concentration in 569B OMVs

A dot blot assay was performed to estimate the CT concentration of the purified 569B OMVs. Two μL of purified CT (Sigma-Aldrich®) in serial dilutions of known concentrations was spotted onto a nitrocellulose membrane. Purified OMVs were then spotted onto the membrane, and the membrane was dried under nitrogen. After incubation with blocking buffer, the OMV-associated CT was detected using the primary and secondary antibodies. A standard curve was plotted for the purified CT spots with known concentration and was used to calculate the concentration of CT in the OMVs. The fractional protein composition of the OMVs (CT/total protein) was then determined by calculating the absorbance at 280 nm (A280) expected for this CT concentration and dividing by the measured A280 of the OMVs.

A dot blot assay was also performed to measure the percentage of OMV-associated CT in the total CT in the culture. The bacteria-free filtered supernatant was concentrated about 20-fold using a PES 10 KDa ultrafiltration centrifugal unit (Pierce; Thermo scientific) to avoid losing any CT. The supernatant was then ultracentrifuged (140,000 × *g*, 3 h, 4°C) using a Beckman SW 55 Ti rotor. The OMV-free supernatant was collected, and the OMV pellet was resuspended in same volume of PBS for further analysis. The samples were concentrated ten-fold using a SpeedVac concentrator (Savant), then two μL of each sample was spotted on a membrane containing a serial dilution of CT as standard. CT was then detected using a polyclonal anti-CT antibody.

4.8 Cytotoxicity assays

The OMV-mediated changes in cell morphology were measured using a cell morphology scoring assay (Massol, Larsen, Fujinaga, Lencer, & Kirchhausen, 2004). Briefly, 4×10^4 of FHs 74 Int cells were grown overnight on a 96-well tissue culture treated plate (CELLSTAR®, Greiner Bio-One). After three washes with Hank's balanced salt solution (HBSS) buffer, cells were treated with 569B OMVs with CT concentrations ranging from 5 ng/well to 40 ng/well for 4 hr, and the morphological changes were measured on a scale of 1 to 4 based on the percentage of cell rounding. Images were captured using a Nikon Eclipse TE2000-U inverted microscope (Nikon Instruments Inc.) at 20× magnification.

To compare the cytotoxicity of OMVs and the OMV-free supernatant, cells were treated with isolated OMVs and OMV-free supernatant diluted in HBSS for 4 hr. Cell rounding was scored accordingly.

In the GM1 competition experiment, the cells were incubated with either OMVs containing 40 ng/well CT or the same mass of OMVs preincubated with GM1 (30 min, 25 °C) in a GM1 to CT ratio of 10:1 for 4 hr.

4.9 LPS purification

LPS was purified from *V. cholerae* 569B using the hot phenol-water extraction method as described before (Westphal, 1965) with some modifications. The cells were centrifuged, and the bacterial pellet was washed twice in PBS. After resuspension in hot water, the sample was boiled for 15 min and then cooled to room temperature. The sample was treated with DNase and RNase (37°C, 1hr) followed by proteinase K (60°C, overnight). Tris-saturated phenol was added to the solution (65°C, 15 min), which was then was cooled on ice and centrifuged (16,000 × *g*, 15 min, 4°C), before the LPS-containing aqueous phase was collected. The phenol phase was incubated again with water (65°C, 15 min), centrifuged again (16,000 × *g*,15 min, 4°C), and the water phase was recovered. The two collected water phases were pooled and dialyzed against DI water and subsequently lyophilized.

After separation by SDS-PAGE on an 8–16% polyacrylamide gel, the LPS samples were stained using the Pro-Q Emerald 300 Lipopolysaccharide Gel Stain Kit (Molecular Probes), according to the manufacturer's instructions.

4.10 Lipid dot blot assay

Two lipid dot blot analyses were performed, as described previously (Munnik & Wierzchowiecka, 2013). On the first nitrocellulose membrane, two μg of POPE, POPG, TOCL, and purified 569B LPS were spotted, and on the second membrane, two μg of the aforementioned lipids along with GM1 were spotted. Both membranes were then dried with nitrogen gas. The membranes were immersed in blocking buffer (5% non-fat dry milk in TBS) for 1 h and then incubated with CT (0.8 μg/mL in blocking buffer) for 1 hr at room temperature. After three washes with TBS, the membranes were incubated with the primary and secondary antibodies, as described above.

4.11 Proteinase K susceptibility assay

The proteinase K digestion assay was performed as previously described (Balsalobre et al., 2006; Cheng & Schneewind, 2000). Briefly, OMVs were treated with proteinase K (1 mg/mL, 30 min, 37°C) either in the absence or presence of 1% SDS. Subsequently, the samples were analyzed by SDS-PAGE and western blotting using a polyclonal anti-CT antibody.

4.12 Indirect non-competitive enzyme-linked immunosorbent assay (ELISA)

The location of the CT on the vesicles was determined using an indirect non-competitive ELISA. Vesicles were treated with 0.1 M EDTA for 2 hr at 37°C to disrupt the membrane. A microtiter ELISA plate (Nunc) was coated with 200 μL of either intact or EDTA-treated

OMVs in triplicate, with CT concentrations ranging from 20 ng/well to 160 ng/well. Three additional wells were incubated with PBS and served as background control. The plate was incubated overnight at room temperature. After three washes with PBS, nonspecific binding was blocked using 3% BSA. Following three washes with PBS, the wells were treated with primary and secondary antibody diluted in BSA. After three final washes, 100 μL of 3,3′, 5,5′-tetramethylbenzidene (TMB) substrate solution (Thermo Fisher Scientific) was added to each well for 15 min. The stop solution (0.16 M sulfuric acid) was then added, and the absorbance at 450 nm was measured using a Tecan microplate reader.

4.13 GM1 ELISA

The GM1 ELISA assay was performed as described previously (Horstman & Kuehn, 2000). Each well of a Maxisorp 96-well microtiter ELISA plate (Nunc) was coated with 100 μL of GM1 ganglioside (1.5 μg/mL in PBS; Sigma-Aldrich®, St. Louis, MO) overnight at room temperature. After three washes with PBS, the non-specific binding sites were blocked by addition of 200 μL of 3% (w/v) fatty acid free bovine serum albumin (BSA). Following three washes, 100 μL of serially diluted samples of either CT, CT preincubated with GM1, 569B OMVs, or 569B OMVs preincubated with GM1 were added to the wells in triplicate and incubated for 2 hr at room temperature with gentle shaking. In each sample, the CT concentration ranged from 80 ng/well to 10 ng/well. In the GM1-treated wells, the CT:GM1 mass ratio was 4:1. The remaining wells were incubated with BSA and served as background control. After three washes with PBS, the plate was incubated with primary and secondary antibody, and the ELISA was developed using TMB solution, as described above.

4.14 Fluorescent labeling of vesicles

The 569B vesicles were fluorescently labeled with fluorescein isothiocyanate (FITC, Sigma-Aldrich®), according to the manufacturer's instructions (Kesty & Kuehn, 2004; Sharpe et al., 2011). The purified vesicles were pelleted (140,000 × *g*, 3 hr) and resuspended in 0.1 M sodium bicarbonate at pH 9. The samples were incubated with FITC and stirred for 1 h at 25°C on a rotator. The free dye was removed from the labeled vesicles by washing twice with PBS (140,000 × *g*, 3 hr).

4.15 Confocal microscopy

For confocal microscopy analysis, 4×10^4 of FHs 74 Int cells were grown overnight on a glass-bottom, poly-L-lysine-coated 96-well plate (ibidi). To label the cell plasma membrane, the wells were coated with 200 μL of 5 μg/mL Alexa Fluor® 555-conjugated WGA (wheat-germ agglutinin; Invitrogen) in HBSS with no phenol red, and incubated at 37°C for 10 min. Following two washes with HBSS, cells were treated with FITC-OMVs or FITC-OMVs preincubated with GM1 (0.4 ng/μL, 30 min, 25°C) in HBSS. After a 2 hr incubation, unbound OMVs were removed, and the cells were washed twice with HBSS. Confocal microscopy was performed using a Nikon C2si+ confocal microscope with a 60x oil immersion objective (NA=1.4). The fluorescence was recorded at wavelengths of 488 nm (green; FITC), and 561 nm (red; Alexa Fluor 555). The images were processed using the ImageJ software.

4.16 Statistical Analysis

Data are presented as mean ± standard deviation (SD) with the indicated sample size. Statistical analysis was performed using an unpaired two-tailed Student's t-test or one-way analysis of variance (ANOVA), followed by the post-hoc Bonferroni test for multiple comparisons. P-values less than 0.05 were considered statistically significant.

Supplementary Material

Refer to Web version on PubMed Central for supplementary material.

Acknowledgments

We thank William Mushock in the Lehigh University Department of Materials Science and Engineering for his assistance with SEM experiments; Will Xia, Ph.D., Lehigh University Health Research Hub (HRH) Manager; and Lee Graham, Lehigh University Department of Biological Sciences Lab Manager. We also thank Mathew Lucas for assistance with vesicle purification. This research has been funded by NSF grant 1554417 and NIH grants DE022795 and DE025275 to ACB.

References

Balakrishnan, VS. Cholera in Yemen. Elsevier; 2017.

Balsalobre C, Silván JM, Berglund S, Mizunoe Y, Uhlin BE, Wai SN. Release of the type I secreted α-haemolysin via outer membrane vesicles from *Escherichia coli*. Molecular Microbiology. 2006; 59(1):99–112. [PubMed: 16359321]

Beddoe T, Paton AW, Le Nours J, Rossjohn J, Paton JC. Structure, biological functions and applications of the AB(5) toxins. Trends in Biochemical Sciences. 2010; 35(7):411–418. DOI: 10.1016/j.tibs.2010.02.003 [PubMed: 20202851]

Bielaszewska M, Ruter C, Bauwens A, Greune L, Jarosch KA, Steil D, … Karch H. Host cell interactions of outer membrane vesicle-associated virulence factors of enterohemorrhagic *Escherichia coli* O157: Intracellular delivery, trafficking and mechanisms of cell injury. Plos Pathogens. 2017; 13(2):51.doi: 10.1371/journal.ppat.1006159

Bielaszewska M, Ruter C, Kunsmann L, Greune L, Bauwens A, Zhang WL, … Karch H. Enterohemorrhagic *Escherichia coli* Hemolysin Employs Outer Membrane Vesicles to Target Mitochondria and Cause Endothelial and Epithelial Apoptosis. Plos Pathogens. 2013; 9(12):30.doi: 10.1371/journal.ppat.1003797

Bomberger JM, MacEachran DP, Coutermarsh BA, Ye S, O'Toole GA, Stanton BA. Long-distance delivery of bacterial virulence factors by *Pseudomonas aeruginosa* outer membrane vesicles. Plos Pathogens. 2009; 5(4):e1000382. [PubMed: 19360133]

Bonnington KE, Kuehn MJ. Protein selection and export via outer membrane vesicles. Biochimica Et Biophysica Acta-Molecular Cell Research. 2014; 1843(8):1612–1619. DOI: 10.1016/j.bbamcr.2013.12.011

Canas MA, Gimenez R, Fabrega MJ, Toloza L, Baldoma L, Badia J. Outer Membrane Vesicles from the Probiotic *Escherichia coli* Nissle 1917 and the Commensal ECOR12 Enter Intestinal Epithelial Cells via Clathrin-Dependent Endocytosis and Elicit Differential Effects on DNA Damage. PLoS One. 2016; 11(8):22.doi: 10.1371/journal.pone.0160374

Chatterjee D, Chaudhuri K. Association of cholera toxin with *Vibrio cholerae* outer membrane vesicles which are internalized by human intestinal epithelial cells. FEBS Letters. 2011; 585(9):1357–1362. [PubMed: 21510946]

Cheng LW, Schneewind O. *Yersinia enterocolitica* TyeA, an intracellular regulator of the type III machinery, is required for specific targeting of YopE, YopH, YopM, and YopN into the cytosol of eukaryotic cells. Journal of Bacteriology. 2000; 182(11):3183–3190. [PubMed: 10809698]

Chinnapen DJF, Chinnapen H, Saslowsky D, Lencer WI. Rafting with cholera toxin: endocytosis and trafficking from plasma membrane to ER. Fems Microbiology Letters. 2007; 266(2):129–137. DOI: 10.1111/j.1574-6968.2006.00545.x [PubMed: 17156122]

Demuth DR, James D, Kowashi Y, Kato S. Interaction of *Actinobacillus actinomycetemcomitans* outer membrane vesicles with HL60 cells does not require leukotoxin. Cellular Microbiology. 2003; 5(2):111–121. [PubMed: 12580947]

Elluri S, Enow C, Vdovikova S, Rompikuntal PK, Dongre M, Carlsson S, … Wai SN. Outer membrane vesicles mediate transport of biologically active *Vibrio cholerae* cytolysin (VCC) from *V. cholerae* strains. PLoS One. 2014; 9(9):13.doi: 10.1371/journal.pone.0106731

Elmi A, Watson E, Sandu P, Gundogdu O, Mills DC, Inglis NF, … Dorrell N. *Campylobacter jejuni* Outer Membrane Vesicles Play an Important Role in Bacterial Interactions with Human Intestinal Epithelial Cells. Infection and Immunity. 2012; 80(12):4089–4098. DOI: 10.1128/iai.00161-12 [PubMed: 22966047]

Faruque SM, Albert MJ, Mekalanos JJ. Epidemiology, genetics, and ecology of toxigenic *Vibrio cholerae*. Microbiology and Molecular Biology Reviews. 1998; 62(4):1301. [PubMed: 9841673]

Hisatsune K, Kondo S, Isshiki Y, Iguchi T, Haishima Y. Occurrence of 2-O-methyl-N-(3-deoxy-L-glycero-tetronyl)-D-perosamine (4-amino-4, 6-dideoxy-D-manno-pyranose) in lipopolysaccharide from Ogawa but not from Inaba O forms of O1 *Vibrio cholerae*. Biochemical and biophysical research communications. 1993; 190(1):302–307. [PubMed: 8422256]

Horstman AL, Kuehn MJ. Enterotoxigenic *Escherichia coli* secretes active heat-labile enterotoxin via outer membrane vesicles. Journal of Biological Chemistry. 2000; 275(17):12489–12496. [PubMed: 10777535]

Horstman AL, Kuehn MJ. Bacterial surface association of heat-labile enterotoxin through lipopolysaccharide after secretion via the general secretory pathway. Journal of Biological Chemistry. 2002; 277(36):32538–32545. DOI: 10.1074/jbc.M203740200 [PubMed: 12087095]

Ito T, Higuchi T, Hirobe M, Hiramatsu K, Yokota T. Identification of a novel sugar, 4-amino-4, 6-dideoxy-2-O-methylmannose in the lipopolysaccharide of *Vibrio cholerae* O1 serotype Ogawa. Carbohydrate research. 1994; 256(1):113–128. [PubMed: 8194067]

Ivers LC. Eliminating cholera transmission in Haiti. New England Journal of Medicine. 2017; 376(2): 101–103. [PubMed: 27959699]

Jin D, Luo Y, Zheng M, Li H, Zhang J, Stampfl M, … Tang Y-W. Quantitative detection of *Vibrio cholerae* toxin by real-time and dynamic cytotoxicity monitoring. Journal of clinical microbiology. 2013; 51(12):3968–3974. [PubMed: 24048535]

Kaparakis-Liaskos M, Ferrero RL. Immune modulation by bacterial outer membrane vesicles. Nature Reviews Immunology. 2015; 15(6):375–387. DOI: 10.1038/nri3837

Kaparakis M, Turnbull L, Carneiro L, Firth S, Coleman HA, Parkington HC, … Ferrero RL. Bacterial membrane vesicles deliver peptidoglycan to NOD1 in epithelial cells. Cellular Microbiology. 2010; 12(3):372–385. DOI: 10.1111/j.1462-5822.2009.01404.x [PubMed: 19888989]

Kato S, Kowashi Y, Demuth DR. Outer membrane-like vesicles secreted by Actinobacillus actinomycetemcomitans are enriched in leukotoxin. Microbial Pathogenesis. 2002; 32(1):1–13. [PubMed: 11782116]

Kesty NC, Kuehn MJ. Incorporation of heterologous outer membrane and periplasmic proteins into *Escherichia coli* outer membrane vesicles. Journal of Biological Chemistry. 2004; 279(3):2069–2076. [PubMed: 14578354]

Kesty NC, Mason KM, Reedy M, Miller SE, Kuehn MJ. Enterotoxigenic *Escherichia coli* vesicles target toxin delivery into mammalian cells. Embo Journal. 2004; 23(23):4538–4549. DOI: 10.1038/sj.emboj.7600471 [PubMed: 15549136]

Kulp, A., Kuehn, MJ. Biological Functions and Biogenesis of Secreted Bacterial Outer Membrane Vesicles. In: Gottesman, S., Harwood, CS., editors. Annual Review of Microbiology. Vol. 64. Palo Alto: Annual Reviews; 2010. p. 163-184.

Kunsmann L, Ruter C, Bauwens A, Greune L, Gluder M, Kemper B, … Bielaszewska M. Virulence from vesicles: Novel mechanisms of host cell injury by *Escherichia coli* O104:H4 outbreak strain. Scientific Reports. 2015; 5:18.doi: 10.1038/srep13252

Kuziemko GM, Stroh M, Stevens RC. Cholera toxin binding affinity and specificity for gangliosides determined by surface plasmon resonance. Biochemistry. 1996; 35(20):6375–6384. [PubMed: 8639583]

Lencer WI, Delp C, Neutra MR, Madara JL. Mechanism of cholera toxin action on a polarized human intestinal epithelial cell line: role of vesicular traffic. Journal of Cell Biology. 1992; 117(6):1197–1209. DOI: 10.1083/jcb.117.6.1197 [PubMed: 1318883]

Lencer WI, Hirst TR, Holmes RK. Membrane traffic and the cellular uptake of cholera toxin. Biochimica Et Biophysica Acta-Molecular Cell Research. 1999; 1450(3):177–190. DOI: 10.1016/s0167-4889(99)00070-1

Lindmark B, Rompikuntal PK, Vaitkevicius K, Song T, Mizunoe Y, Uhlin BE, … Wai SN. Outer membrane vesicle-mediated release of cytolethal distending toxin (CDT) from *Campylobacter jejuni*. BMC microbiology. 2009; 9(1):220. [PubMed: 19835618]

Masserini M, Freire E, Palestini P, Calappi E, Tettamanti G. Fuc-GM1 ganglioside mimics the receptor function of GM1 for cholera toxin. Biochemistry. 1992; 31(8):2422–2426. [PubMed: 1311601]

Massol RH, Larsen JE, Fujinaga Y, Lencer WI, Kirchhausen T. Cholera toxin toxicity does not require functional Arf6-and dynamin-dependent endocytic pathways. Molecular Biology of the Cell. 2004; 15(8):3631–3641. DOI: 10.1091/mbc.E04-04-0283 [PubMed: 15146065]

Matson JS, Withey JH, DiRita VJ. Regulatory networks controlling *Vibrio cholerae* virulence gene expression. Infection and Immunity. 2007; 75(12):5542–5549. DOI: 10.1128/iai.01094-07 [PubMed: 17875629]

Mondal A, Tapader R, Chatterjee NS, Ghosh A, Sinha R, Koley H, … Pal A. Cytotoxic and Inflammatory Responses Induced by Outer Membrane Vesicle-Associated Biologically Active Proteases from *Vibrio cholerae*. Infection and Immunity. 2016; 84(5):1478–1490. DOI: 10.1128/iai.01365-15 [PubMed: 26930702]

Munnik T, Wierzchowiecka M. Lipid-binding analysis using a fat blot assay. Plant Lipid Signaling Protocols. 2013:253–259.

O'Donoghue EJ, Krachler AM. Mechanisms of outer membrane vesicle entry into host cells. Cellular Microbiology. 2016; 18(11):1508–1517. DOI: 10.1111/cmi.12655 [PubMed: 27529760]

Parker H, Chitcholtan K, Hampton MB, Keenan JI. Uptake of *Helicobacter pylori* Outer Membrane Vesicles by Gastric Epithelial Cells. Infection and Immunity. 2010; 78(12):5054–5061. DOI: 10.1128/iai.00299-10 [PubMed: 20876296]

Peek JA, Taylor RK. Characterization of a periplasmic thiol: disulfide interchange protein required for the functional maturation of secreted virulence factors of *Vibrio cholerae*. Proceedings of the National Academy of Sciences of the United States of America. 1992; 89(13):6210–6214. DOI: 10.1073/pnas.89.13.6210 [PubMed: 1631111]

Reidl J, Klose KE. *Vibrio cholerae* and cholera: out of the water and into the host. Fems Microbiology Reviews. 2002; 26(2):125–139. DOI: 10.1111/j.1574-6976.2002.tb00605.x [PubMed: 12069878]

Rompikuntal PK, Thay B, Khan MK, Alanko J, Penttinen AM, Asikainen S, … Oscarsson J. Perinuclear Localization of Internalized Outer Membrane Vesicles Carrying Active Cytolethal Distending Toxin from Aggregatibacter actinomycetemcomitans. Infection and Immunity. 2012; 80(1):31–42. DOI: 10.1128/iai.06069-11 [PubMed: 22025516]

Sanchez J, Holmgren J. Cholera toxin - A foe & a friend. Indian Journal of Medical Research. 2011; 133(2):153–163. [PubMed: 21415489]

Sandkvist M. Biology of type II secretion. Molecular Microbiology. 2001a; 40(2):271–283. DOI: 10.1046/j.1365-2958.2001.02403.x [PubMed: 11309111]

Sandkvist M. Type II secretion and pathogenesis. Infection and Immunity. 2001b; 69(6):3523–3535. DOI: 10.1128/iai.69.6.3523-3535.2001 [PubMed: 11349009]

Sandkvist M, Michel LO, Hough LP, Morales VM, Bagdasarian M, Koomey M, … Bagdasarian M. General secretion pathway (eps) genes required for toxin secretion and outer membrane biogenesis in *Vibrio cholerae*. Journal of Bacteriology. 1997; 179(22):6994–7003. [PubMed: 9371445]

Schild S, Nelson EJ, Camilli A. Immunization with *Vibrio cholerae* outer membrane vesicles induces protective immunity in mice. Infection and Immunity. 2008; 76(10):4554–4563. DOI: 10.1128/iai.00532-08 [PubMed: 18678672]

Schwechheimer C, Kuehn MJ. Outer-membrane vesicles from Gram-negative bacteria: biogenesis and functions. Nature Reviews Microbiology. 2015; 13(10):605–619. DOI: 10.1038/nrmicro3525 [PubMed: 26373371]

Sharpe SW, Kuehn MJ, Mason KM. Elicitation of Epithelial Cell-Derived Immune Effectors by Outer Membrane Vesicles of Nontypeable Haemophilus influenzae. Infection and Immunity. 2011; 79(11):4361–4369. DOI: 10.1128/iai.05332-11 [PubMed: 21875967]

Shaw C, Taylor R. *Vibrio cholerae* O395 tcpA pilin gene sequence and comparison of predicted protein structural features to those of type 4 pilins. Infection and Immunity. 1990; 58(9):3042–3049. [PubMed: 1974887]

Sikora AE. Proteins Secreted via the Type II Secretion System: Smart Strategies of *Vibrio cholerae* to Maintain Fitness in Different Ecological Niches. Plos Pathogens. 2013; 9(2):4.doi: 10.1371/journal.ppat.1003126

Spangler BD. Structure and function of cholera toxin and the related *Escherichia coli* heat-labile enterotoxin. Microbiological Reviews. 1992; 56(4):622–647. [PubMed: 1480112]

Stroeher UH, Karageorgos LE, Morona R, Manning PA. Serotype conversion in *Vibrio cholerae* O1. Proceedings of the National Academy of Sciences. 1992; 89(7):2566–2570.

Tauschek M, Gorrell RJ, Strugnell RA, Robins-Browne RM. Identification of a protein secretory pathway for the secretion of heat-labile enterotoxin by an enterotoxigenic strain of *Escherichia coli*. Proceedings of the National Academy of Sciences of the United States of America. 2002; 99(10):7066–7071. DOI: 10.1073/pnas.092152899 [PubMed: 12011463]

Taylor M, Banerjee T, Ray S, Tatulian SA, Teter K. Protein-disulfide Isomerase Displaces the Cholera Toxin A1 Subunit from the Holotoxin without Unfolding the A1 Subunit. Journal of Biological Chemistry. 2011; 286(25):22090–22100. DOI: 10.1074/jbc.M111.237966 [PubMed: 21543321]

Villeneuve S, Boutonnier A, Mulard LA, Fournier JM. Immunochemical characterization of an Ogawa-Inaba common antigenic determinant of *Vibrio cholerae* O1. Microbiology. 1999; 145(9): 2477–2484. [PubMed: 10517600]

Wernick NLB, Chinnapen DJF, Cho JA, Lencer WI. Cholera Toxin: An Intracellular Journey into the Cytosol by Way of the Endoplasmic Reticulum. Toxins. 2010; 2(3):310–325. DOI: 10.3390/toxins2030310 [PubMed: 22069586]

Westphal O. Bacterial lipopolysaccharides: extraction with phenol-water and further application of the procedure. Methods Carbohydr Chem. 1965; 5:83–89.

Yu J, Webb H, Hirst TR. A homologue of the *Escherichia coli* DsbA protein involved in disulphide bond formation is required for enterotoxin biogenesis in *Vibrio cholerae*. Molecular Microbiology. 1992; 6(14):1949–1958. DOI: 10.1111/j.1365-2958.1992.tb01368.x [PubMed: 1324389]

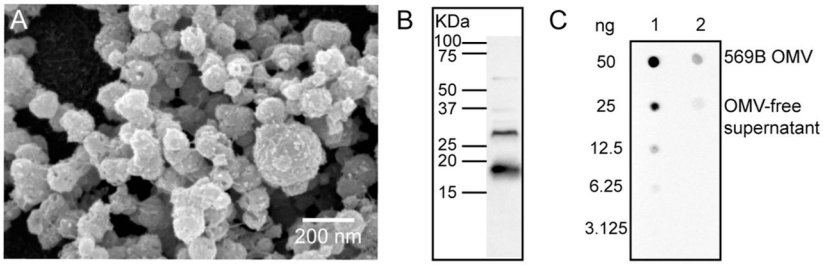

FIGURE 1. Characterization of *V. cholerae* OMVs

(A) Scanning electron micrographs of *V. cholerae* 569B OMVs. (B) Western blot analysis of *V. cholerae* 569B OMVs. Two strong anti-CT polyclonal antibody-reactive bands were detected, demonstrating the presence of CT in the OMVs. (C) Relative CT concentration in 569B OMVs and OMV-free supernatant. The mass of CT present in purified OMVs or the OMV-free supernatant was determined by comparing the intensity of an antibody-reactive spot to that of CT standards with known mass.

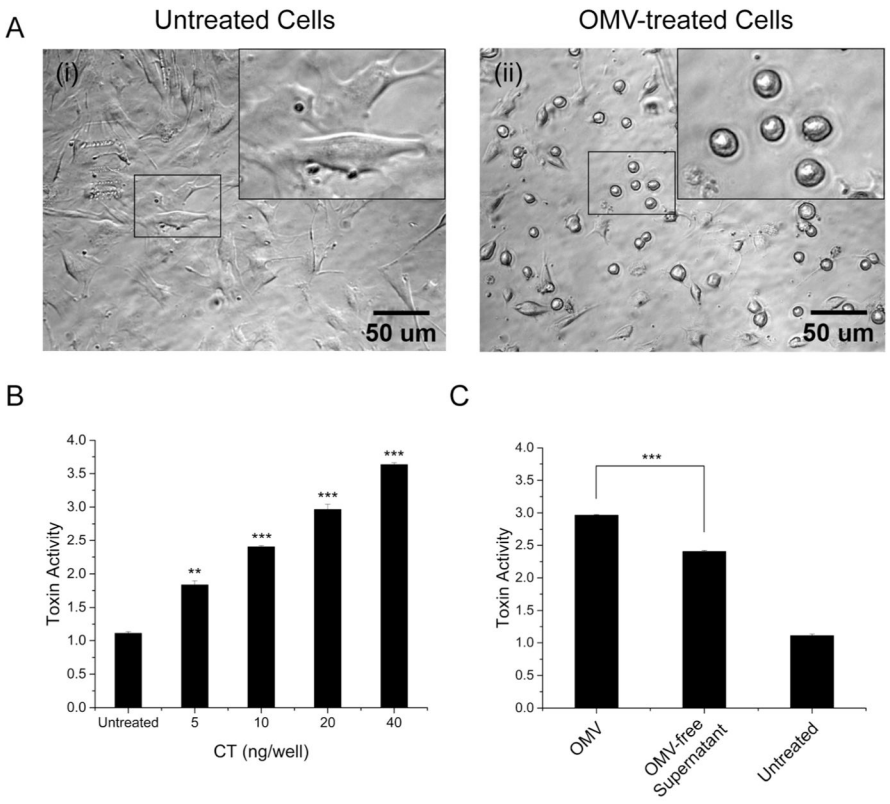

FIGURE 2. ***V. cholerae*** **569B OMV-mediated cytotoxicity**

(A) Representative phase contrast image of OMV-treated FHs 74 intestinal epithelial cells. (i) Untreated cells and (ii) OMV-treated cells (0.4 ng/μL of CT, 4 hr). Enlarged view of the regions in small boxes are shown in the insets. (B) Quantitative analysis of the OMV-treated cell morphology. Cells were treated with a serial dilution of 569B OMVs (5 to 40 ng CT/well), and the resulting morphology scored on a scale of 1 (spindly) to 4 (rounded), based on the percentage of cell rounding. Data are expressed as mean ± SD (N=3). One-way ANOVA followed by Bonferroni's post hoc test was used to compare differences between treated and untreated samples. * $p < 0.05$, ** $p < 0.01$, and *** $p < 0.001$. (C) Quantification of 569B OMV- and OMV-free supernatant-mediated cytotoxicity. Cells were treated with purified OMVs or OMV-free supernatant. Control cells were treated with HBSS. OMV-mediated alterations in cell morphology were scored on a scale of 1 (spindly) to 4 (rounded). Data are expressed as mean ± SD (N=3). The level of significance was determined between cells treated with OMVs and OMV-free supernatant using an unpaired two-tailed t-test. *** $p < 0.001$.

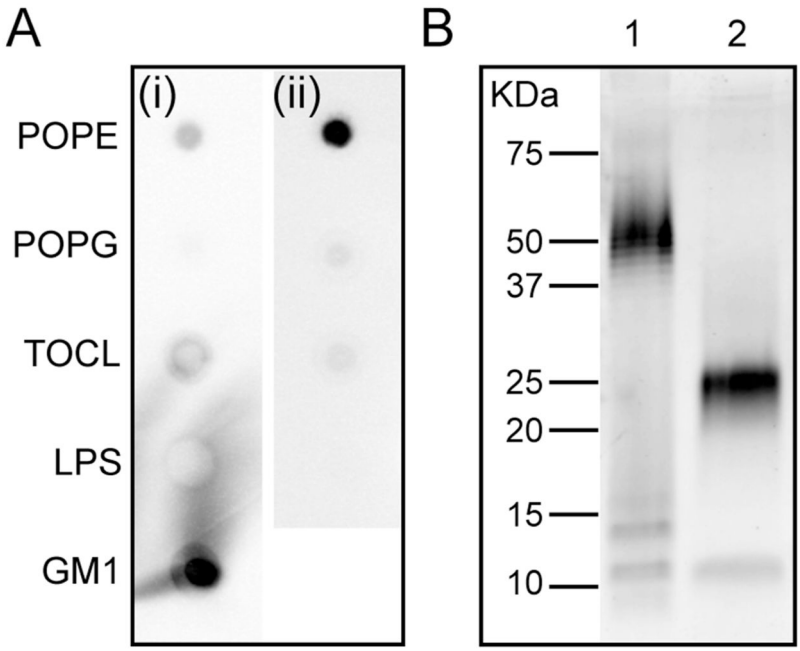

FIGURE 3. Characterization of soluble CT association with OMV lipids

(A) Lipid dot blot analysis of CT affinity for (i) POPE, POPG, TOCL, 569B LPS and GM1, and (ii) POPE, POPG, TOCL, and 569B LPS (with no GM1). In the presence of GM1, free CT was found to have strong affinity for GM1, and in absence of GM1, it had some affinity for POPE. In both cases no affinity for 569B LPS was seen. (B) SDS-PAGE analysis of purified LPS from *V. cholerae* 569B. Lane 1 is the LPS standard and lane 2 is 569B LPS.

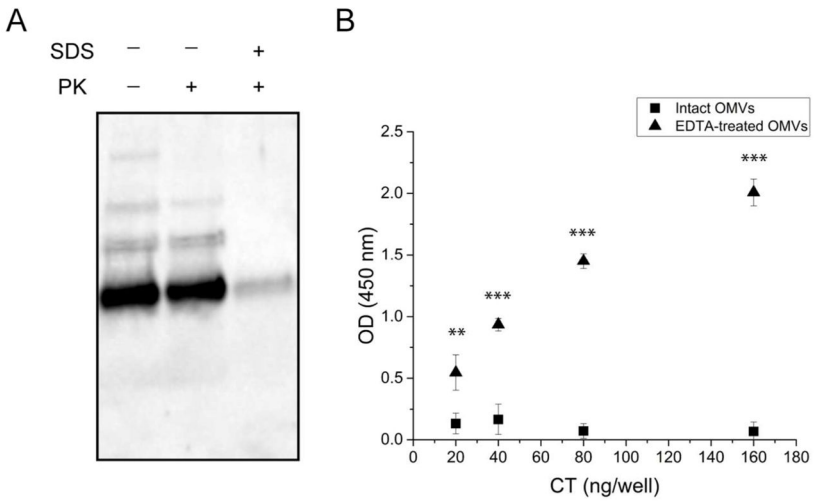

FIGURE 4. Localization of OMV-associated CT

(A) Proteinase K digestion of 569B OMVs. Lane 1: untreated OMVs. Lane 2: Proteinase K-treated OMVs. Lane 3: SDS- and proteinase K-treated OMVs. (B) Indirect noncompetitive ELISA of intact (squares) and EDTA-treated (triangles) 569B OMVs. EDTA-disrupted OMVs bound to the anti-CT polyclonal antibody-coated plate, but intact OMVs did not. Data are shown as mean + SD (N=3). The level of significance was determined using one-way ANOVA followed by Bonferroni's multiple comparison test showing a statistically significant difference between intact and EDTA-treated 569B OMVs. ** $p < 0.01$ and *** $p < 0.001$.

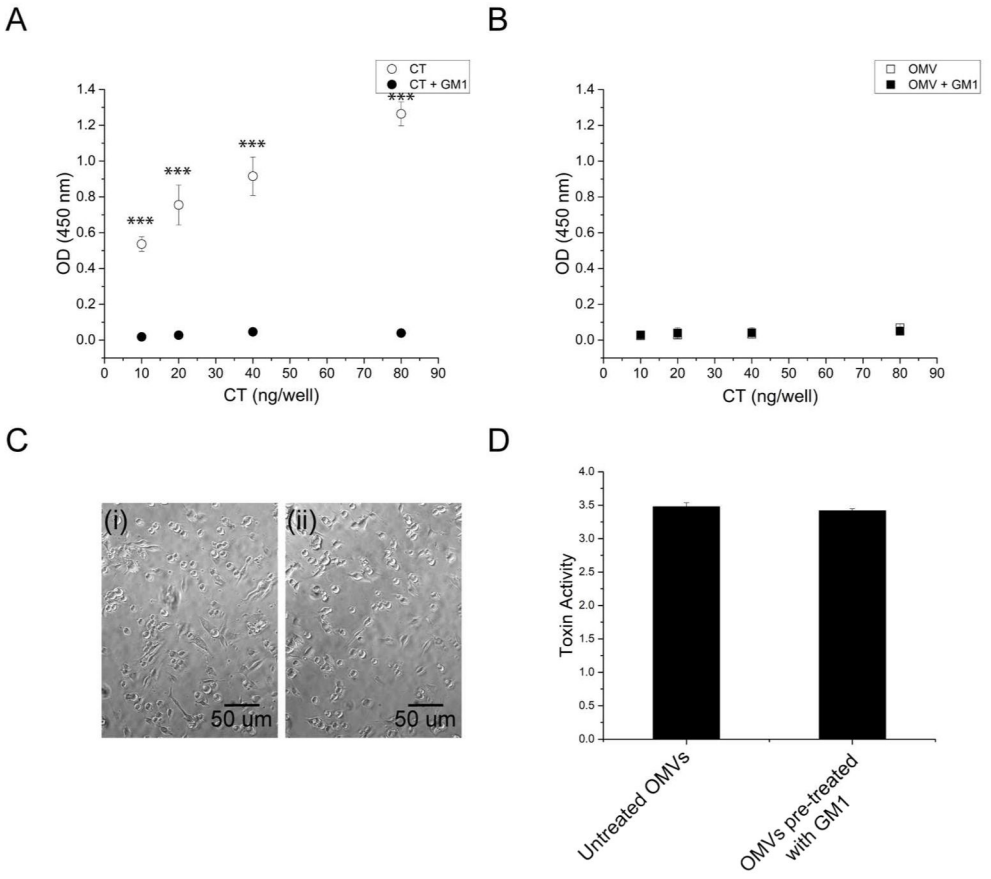

FIGURE 5. 569B OMV association with GM1

(A) GM1 ELISA to measure soluble CT binding to GM1. Soluble CT (open circles) binds to coated GM1; CT pretreated with GM1 (filled circles) does not bind GM1. Data are shown as mean ± SD (N=3). The level of significance was determined using one-way ANOVA followed by Bonferroni's multiple comparison test. (B) GM1 ELISA to measure OMV binding to GM1. Neither OMVs (open squares) nor GM1-treated OMVs (filled squares) bind GM1. Data are expressed as mean ± SD (N=3). One-way ANOVA analysis indicated no significant difference between untreated and GM1-treated OMVs. (C) Phase contrast image of FHs 74 intestinal epithelial cells treated with OMVs. (i) Untreated OMVs and (ii) GM1-pretreated OMVs (0.4 ng/μL of CT, 4 hr). Both untreated and GM1-treated OMVs induce cell rounding. (D) Quantitative analysis of the morphology of cells treated with untreated OMVs or OMVs pre-treated with GM1. Data are expressed as mean ± SD (N=3). No significant difference was observed between two samples as determined by an unpaired two-tailed t-test.

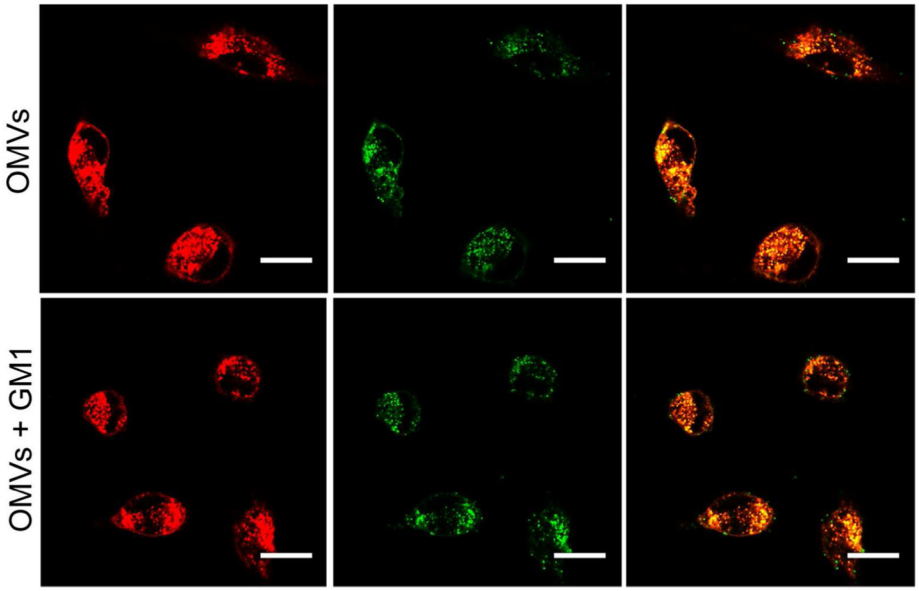

FIGURE 6. GM1-dependence of cellular association of OMVs

FHs 74 intestinal epithelial cells were labeled with AF555-WGA (red) and 569B OMVs were labeled with FITC (green). Both untreated (top) and GM1-treated OMVs (bottom) are associated with host cells within two hrs. The scale bar in all the figures is 5 μm.

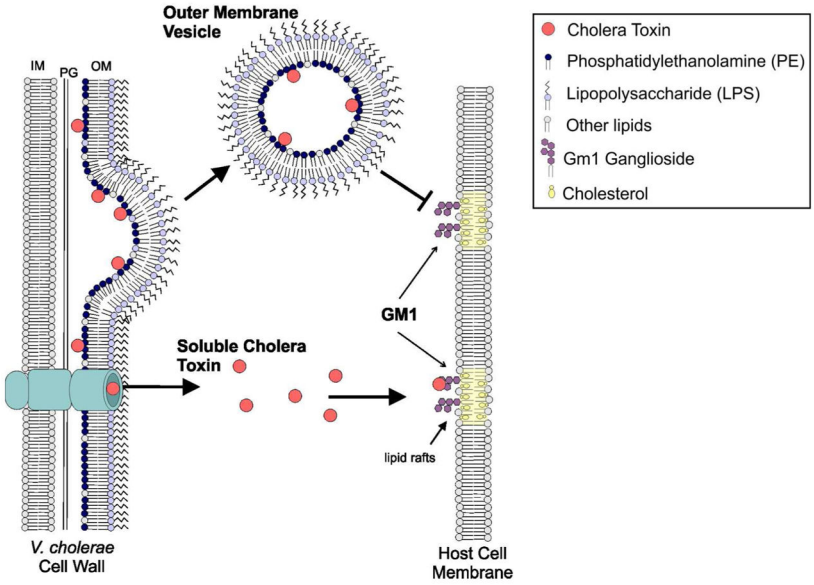

FIGURE 7. Schematic of proposed mechanism of CT association with 569B OMVs

Our results demonstrate that CT has no affinity for LPS, which comprises the outer leaflet of the OM, and resides entirely within the lumen of the OMVs. We therefore hypothesize that during T2S, some CT remains in the periplasm, allowing it to become incorporated in the OMV lumen. Unlike soluble CT, OMV-associated CT does not bind to the GM1 receptor in the lipid rafts of the host cell membrane because of the toxin's location within the OMV. We propose that CT secretion via OMVs and through the T2S system are therefore complementary mechanisms for CT delivery.